CHAPTER IV
ORGANOMODIFIED BENTONITE CONTENTS INFLUENCED PROPERTIES OF PP/ORGANOMODIFIED BENTONITE NANOCOMPOSITE PACKAGING FILMS

4.1 Abstract

Na-bentonite was treated with a surfactant (StepantexTM SP-90) in order to prepare organobentonite, and 3-aminopropyltrimethoxysilane was also added to act as surface treatment. This organomodified-BTN was incorporated into polypropylene with a compatibilizer (Surlyn® ionomer) in a twin screw extruder and fabricated into films by the blow film extrusion process. incorporated into polypropylene with a compatibilizer (Surlyn® ionomer) in a twin screw extruder and fabricated into films by the blow film extrusion process. The organomodified-BTN was characterized by XRD and FTIR. The d-spacing of the organoclay increased when the surfactant was added and the C=O bond and $-CH_2$ of the surfactant occurred at 1740 and 2921 cm^{-1}, respectively. The degradation temperatures of those films were improved. The mechanical properties of the nanocomposite films were also investigated. When the present clay content of the organomodified-BTN was increased, it enhanced the elastic modulus but decreased other tensile properties. The gas permeability of nanocomposites films are reduced when compare with polypropylene films.

4.2 Introduction

One of the most commonly found problems of the horticaltural products is the decreasing of their quality with storage or holding time. Because fruits and vegetables are perishable products with active metabolism during the post harvest, so packaging plays an important role in maximizing the shelf life of both the handling and preservation approaches to shelf life extension. However, traditional-packaging concepts are limited in their ability, thus, the new food packaging has been introduced as a response to the continuous changes in consumer demand and market trends for better quality, mildly preserved, fresh-like, tasty, and convenient food products. In addition, the changing of retail and distribution practices such as centralization of activities, new trends, and globalization of markets, resulting in

increased distribution distances with longer storage times and different temperature requirements for a set of different products, present major challenges and huge demand on food packaging industry. Therefore, the variety of active packaging technologies have been developed in order to extend shelf life while the packaged food maintain safety and quality as well. Important active packaging systems include carbon dioxide emitter/absorbers, moisture absorbers, ethylene absorbers, ethanol emitters, flavor releasing/absorbing systems, time-temperature indicators, and antimicrobial containing films.

The main problems of fresh fruits and vegetables are both ethylene and carbon dioxide gas. Ethylene (C_2H_4) is a growth-simulating hormone that has difference physiological effects on fruits and vegetables. It accelerates softening, ripening, and senescence by increasing the respiration rate, thereby decreasing shelf life. Ethylene also accelerate the rate of chlorophyll degradation, in other words, it can cause yellowing of green vegetables. Hence, ethylene gas is removed from the package headspace to slow senescence and prolong shelf life. For carbon dioxide (CO_2) gas, it is formed due to deterioration and respiration reactions. The produced CO_2 should be removed from the package to avoid food deterioration and gas pressure built up inside rigid packaging or volume expansion in flexible packaging.

Several techniques have been developed to prolong shelf life of fresh fruits and vegetables. Most of these are supplied as sachets or integrated into films. The most well-know, cheap, and extensively used ethylene absorbing system consists of potassium permanganate ($KMnO_4$) imbedded in an inert carrier with a large surface area. However, potassium permanganate cannot be integrated into food-contact surfaces of packaging films, but are supplied only as sachets due to their toxicity. Another ethylene scavenger is based on the absorption of ethylene on activated carbon and subsequent breakdown by metal catalyst, such as charcoal and palladium chloride. Incidentally, for carbon dioxide scavengers, they are commercialized as a sachet, such as the active compound $Ca(OH)_2$ of FreshLock®. Moreover, they can be composed of other physical absorbent (zeolite or active carbon powder), or a chemical absorbent (Na_2CO_3, $Mg(OH)_2$, etc.). In addition, the other absorbing technologies are based on the dispersed minerals (clays), which are embedded in polymer bags, and then used for fresh products.

Last year, Varothai Y. *et al.* studied PP/organoclay films. They used aluminum hydroxide and aluminum acetate as ethylene scavenger in the active

packaging films. However, the purpose of this work is also to prepare ethylene and carbon dioxide scavenger film based on PP/modified clay. Clay minerals, Bentonite, were treated for exfoliated the clay platelets by surfactant (Stepantex-90). The ethylene and carbon dioxide scavengers are aluminum hydroxide and calcium hydroxide, respectively. The ethylene scavenger was attached to nanoclay by using 3-aminopropyl-trimethoxysilane to act as surface treatment to stabilize the exfoliatated state of organoclay, and then, compound with polypropylene to be nanocomposite pellets. However, carbon dioxide scavenger is incorporated with polypropylene by melt intercalation. Both of them are fabricated to be active packaging films. In addition, X-ray Diffractometer (XRD), Scanning Electron Microscope (SEM), Fourier Transform Infrared Spectroscopy (FT-IR), and Thermogravimetric Analysis (TGA), was used for characterize this film. Mechanical properties, permeability, ethylene and carbon dioxide adsorption, and thermal properties of the obtained film were also investigated.

4.3 Experimental

A. Materials

Commercial sodium activated bentonite Mac-Gel® (GRADE SAC), Na-BTN, with cationic exchange capacitor (CEC) of 44.5 meq/100 g clay, was supplied by Thai Nippon Co., Ltd. Thailand. For the surfactant, dipalmitoylethyl hydroxyethyl monium methosulfate (Stepantex™ SP-90), was received from Sunny World Co., Ltd. Moreover, ethanol 99.8% v/v was purchased from Carlo Erba, and polypropylene (Polene 1126 NK, MFI =11 dg/min) was commercially purchased from IRPC Public Co., Ltd. Thailand. The compatibilizer, Sodium-neutralized ethylene-co-methacrylic acid (Surlyn® PC350, MFI=4.5 dg/min), was supplied by DuPont (Thailand) Co. Ltd

B. Preparation of organo-modified bentonite

350g of Na-bentonite is swollen in 10L water for 24 hours. Alkyl ammonium ion (DOEM) is dissolved in 1600 ml solution of water/ethanol (1v/v) at 80°C for 30 min. The swollen clay and alkyl ammonium ion solution are mixed together at 80°C for 2 hr with vigorously stirring, and follow by homogenized for 30 min. Then, the mixture is filtrated and washed with hot water several times. After that, it is dried in a

vacuum oven overnight at 100°C and ground into powder through a sieve, 325 mesh [1].

The interlayer spacing of organomodified-BTN were obtained with XRD of a Rigaku Model Dmax 2002 performed at 2Θ range of 2-40 degrees with scan speed 2 degree/min and scan step 0.01 degree.

Thermal properties of organomodified-BTN were investigated using TGA from Perkin-Elmer Pyris Diamond TG/DTA instrument under N_2 flow of 200 ml/min. The heating process was conducted from 30-900°C at a rate of 10°C/min.

The FT-IR spectra of organoclay were collected from a Nicolet Nexus 670 FT-IR spectrometer with a wave number between 4,000-500 cm^{-1} and 32 scans at a resolution of 2 cm^{-1}.

C. Preparation of PP/organo-modified bentonite nanocomposite films

The master batches containing 50 wt% organomodified clays with compatibilizer, Surlyn®, were firstly prepared. Then, the various contents of organomodified clays (1, 3 and 5 %wt), was compounded with PP to obtained 1%, 3%, and 5% wt of organoclay nanocomposites pellets using a Model T-20 co-rotating twin-screw extruder (Collin) with L/D=30 and D=25 mm. The operating temperatures of extruder were performed at 80, 170, 180, 190, 200, and 210°C from hopper to die, respectively, with 50 rpm of screw speed. After that, these nanocomposites pellets were dried under vacuum at 80°C and fabricated into the packaging film by tubular blown film extrusion process. The screw speed was 50 rpm, screw diameter was 45 mm, L/D was 26 and the processing temperature were 210°C from hopper to die.

The clay contents of the nanocomposite films were determined by a Perkin-Elmer Pyris Diamond TG/DTA Analyzer. Moreover, crystallization and melting behavior of PP that incorporate with organoclay were investigated by Perkin-Elmer DSC 7 analyzer. The heat flow and temperature of the instrument were calibrated by indium which is a standard material. Nitrogen was consistently purged within the equipment to prevent specimens from thermal degradation. The specimens were first melted at 200°C, then, cooled down to room temperature at 10°C/min rate and they were also heated at 10°C/min for the corresponding melting behavior investigations.

The crystal structure of nanocomposites films were performed with XRD of a Rigaku Model Dmax 2002 performed at 2Θ range of 10-30 degrees with scan speed 2 degree/min and scan step 0.01 degree.

The dispersion of clay particles in the PP matrix was investigated by scanning electron microscopy using JEOL JSM-5410 LV Model. The selected specimens, which were nanocomposite and PP pellets, were dipped and fractured in liquid nitrogen. Then, the specimens were coated with gold under vacuum to make them electrically conductive before viewing under a scanning electron microscope (SEM) operating at 15 kV.

The tensile tests were conducted as ASTM D882 with Lloyd universal testing machine. Modulus is measured by extensometer at a crosshead speed 50 mm/min and load cell 500N. The specimens are cut into rectangular shape with 10x100 mm and the experiments are taken under room temperature without preconditioning of the samples.

The oxygen gas permeability was measured according to ASTM D1434 by Oxygen Permeation Analyser Model 8000, Illinois Instrument Inc. , at 23°C with flow rate of N_2 23 cc/min and O_2 50 cc/min. The films were prepared from a compression-molded sheet with the same thickness of 150 μm and were cut into circular shape with 15 cm in diameter.

4.4 Results and Discussion

A. Characterizations of the organomodified bentonite

The X-ray diffraction (XRD) pattern of Na-BTN, organomodified-BTN which is referred to Na-BTN that treated with surfactant (Stepantex^{TM} SP-90) , and organomodified-BTN treated with 3-aminopropyltrimethoxysilane are shown in Figure 4.1. It reveals that the d_{001} peak of pristine Na-BTN at 2Θ = 7.6° corresponds to basal spacing of 1.16 nm (Figure 4.1 a). For the organomodified-BTN, d_{001} observed at 2Θ = 4.42° and 5.92° which are 1.99 and 1.49 nm, respectively. This modified bentonite shows broad peaks at the lower angles due to the inhomogeneous distribution of the surfactant between the layers of the clay, presenting a broader range of interlayer distances depending on the extent of ion exchange [2]. Also, the organoclay treated with silane, shows a sharp peak at 2Θ = 5.04° which has basal spacing of 1.75.
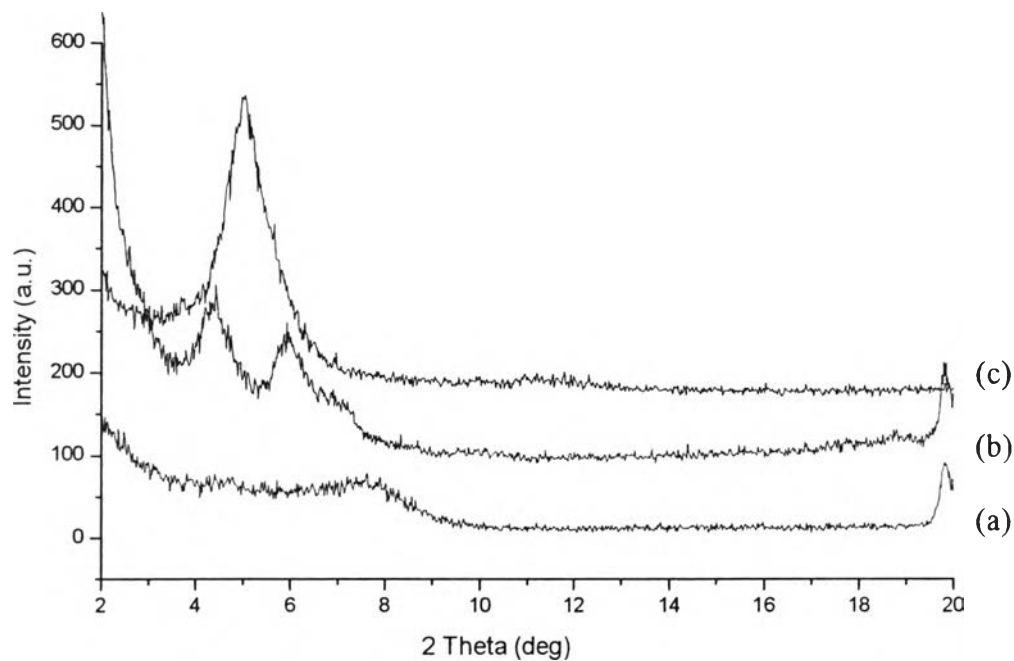
Figure 4.1 The XRD patterns: (a) Na-BTN, (b) Organomodified-BTN, and (c) Organomodified-BTN treated with silane

Moreover, the presence of the surfactant can be observed by fourier transform infrared spectra (FT-IR) between the wave number of 4000 - 500 cm^{-1}. Figure 4.2 shows the FT-IR spectra of Na-BTN, organomodified-BTN, and organomodified-BTN treated with silane. The peak at 2852 and 2921 cm^{-1} are corresponded to the symmetric and asymmetric stretching vibration of the methyl group in the surfactant molecules. Furthermore, Na-BTN which is modified with surfactant, it also contains ether group. Thus, the stretching vibration of the carbonyl group (>C=O) has the absorption peak at 1740 cm^{-1}. At 1090-1015 cm^{-1}, this region shows the Si-O-Si bond of all samples [3].
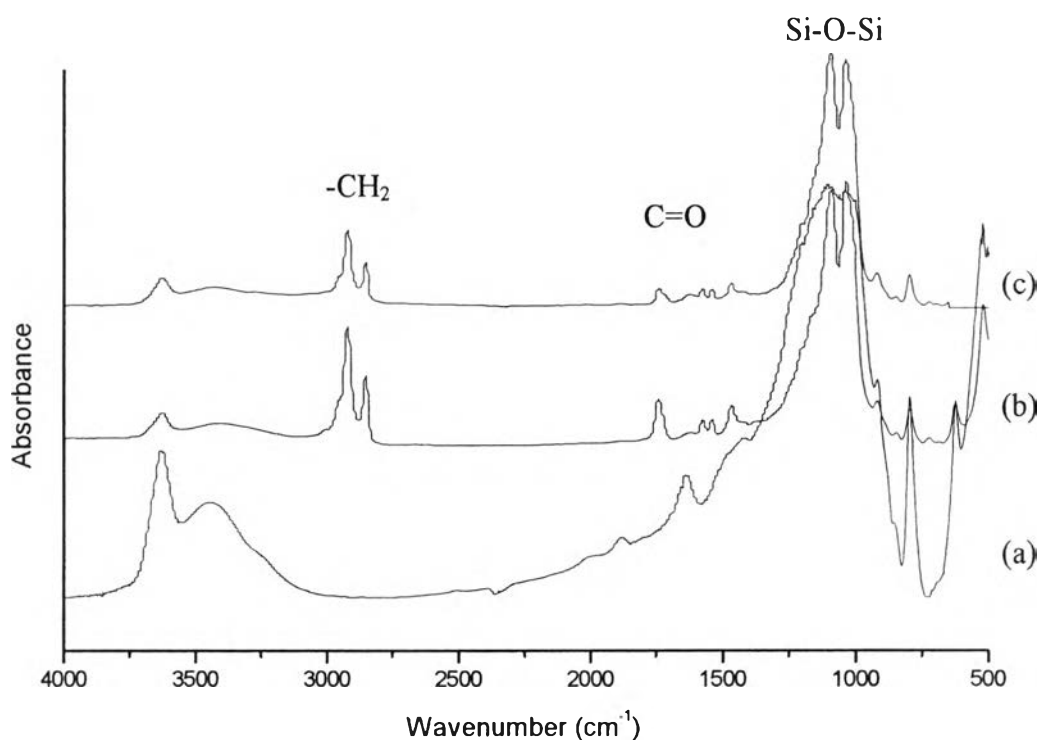
Figure 4.2 Infrared spectra of organobentonite: (a) Na-BTN, (b) Organomodified-BTN, and (c) Organomodified-BTN treated with silane

The thermogravimetric analysis (TGA) of Na-BTN, organomodified-BTN and organomodified-BTN treated with silane are shown in Table 4.1 which is determined the content of the organic component from the weight loss. For pure Na-BTN, it is related to the structural -OH unit of clay at the step of 654.17 $^{\circ}$C and mass loss about ~1.14%. For organomodified-BTN, the weight loss started around 270 to 370°C, corresponding to thermal decomposition of the surfactant [4]. In addition, the TGA curve of organoclay treated with silane exhibit three main composition regions. At region between 200 - 600°C, which corresponds to the thermal decomposition of the organic molecule, is considered for silane coverage.

Table 4.1 Thermal behavior of organobentonite

Sample	Mass Loss H$_2$O (wt%)	Mass Surfactant (wt%)	Char Residual (wt%)	Desurfactant		
				T$_d$ (°C)	T$_i$ (°C)	T$_f$ (°C)
Na-BTN	-	-	98.33	-	-	-
Organomodified-BTN	0	35.4	64.3	336.8	270.8	367.8
Organomodified-BTN treated with silane	1.1	27.7	28.8	376.9	185.6	391.7

B. Thermal behavior of PP/organobentontie nanocomposite films

The differential scanning calorimeter (DSC) was measured in the range of 30-200°C to determine the melting and crystallization behavior of PP and PP/organoclay nanocomposite films as shown in Table 4.2 and Figure 4.3. From the results, melting temperature and crystallization temperature of organomodified-BTN nanocomposites films were higher than pure PP. Moreover, the results show that PP/organoclay nanocoposite films present higher % crystallinity, than pure PP. Because, organoclay acts as nucleating agent. However, 5 wt% content of organoclay was lower than other percent due to the aggregation of organo-modified clay leading to the obstruction of the packing of the crystalline [5].

Table 4.2 Melting and crystallization behavior of PP and PP/organoclay nanocomposite films

Sample	T$_{c, peak}$ (°C)	T$_{m, peak}$ (°C)	ΔH_m (J/g)	% crystallinity
PP	108.63	158.37	69.46	33.23
PP/6%Surlyn	113.3	159.7	73.46	37.39
PP/6%Surlyn/1%Clay	109.97	159.2	66.10	34.01
PP/6%Surlyn/3%Clay	110.3	158.87	64.61	33.97
PP/6%Surlyn/5%Clay	112.3	159.2	61.59	33.11

(PP at 100% crytallinity, ΔH_m = 209 J/g)
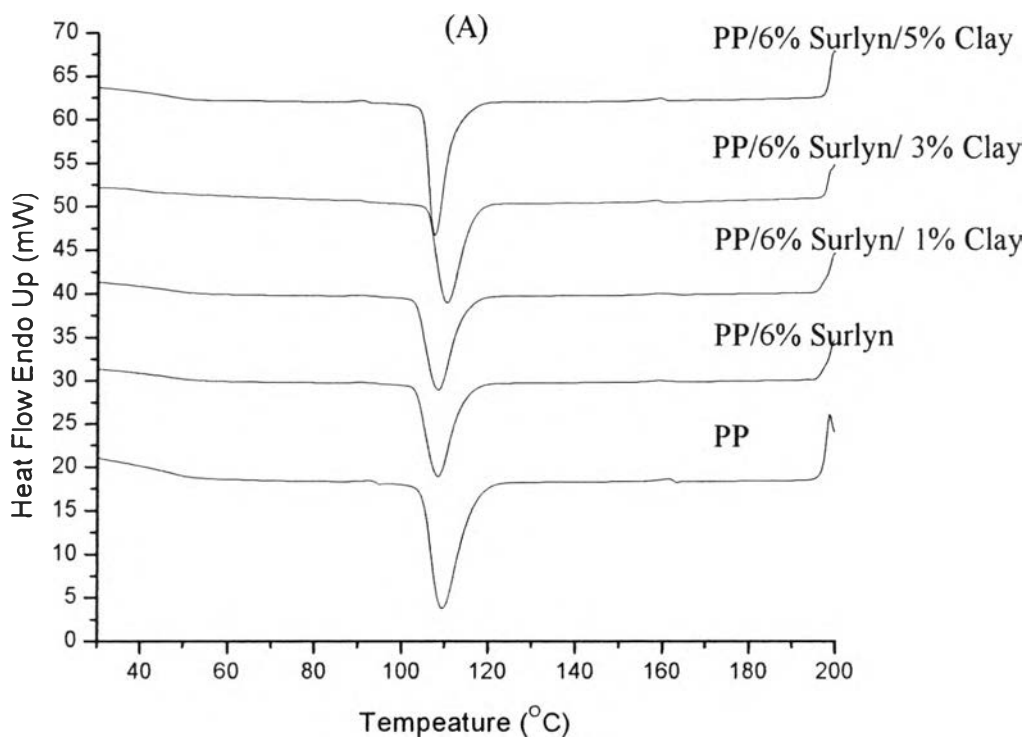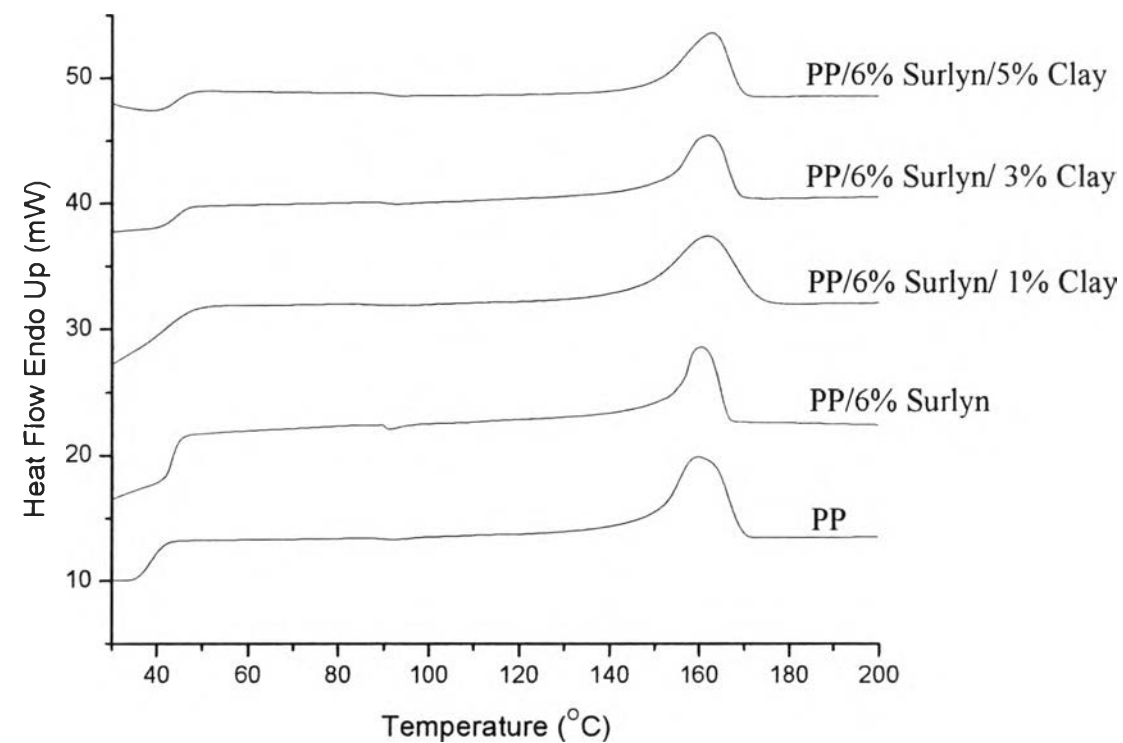
Figure 4.3 DSC thermograms of PP/organoclay nanocomposites film (A) Melting Temperature, and (B) Crystallization Temperature.

Furthermore, the thermogravimetric analysis (TGA) is carried out to investigate the change in weight loss at different temperature. As Table 4.3, when organomodified-BTN is incorporated into PP, it can improve the degradation temperature or thermal stability, according to the presence of metal oxides in organoclay such as silica, aluminium and magnesium [6].

Table 4.3 Thermal behavior of PP and PP/organoclay nanocomposites film

Sample	TGA			
	Clay Content (wt%)	T_d (°C)	T_i (°C)	T_f (°C)
PP	-	443.7	420.5	453.7
PP/Surlyn	6.6	444.3	429.0	456.6
PP/Surlyn/1%Clay	6.7	445.7	428.4	455.3
PP/Surlyn/3%Clay	7.1	446.6	427.0	456.1
PP/Surlyn/5%Clay	11.3	447.6	427.2	457.1
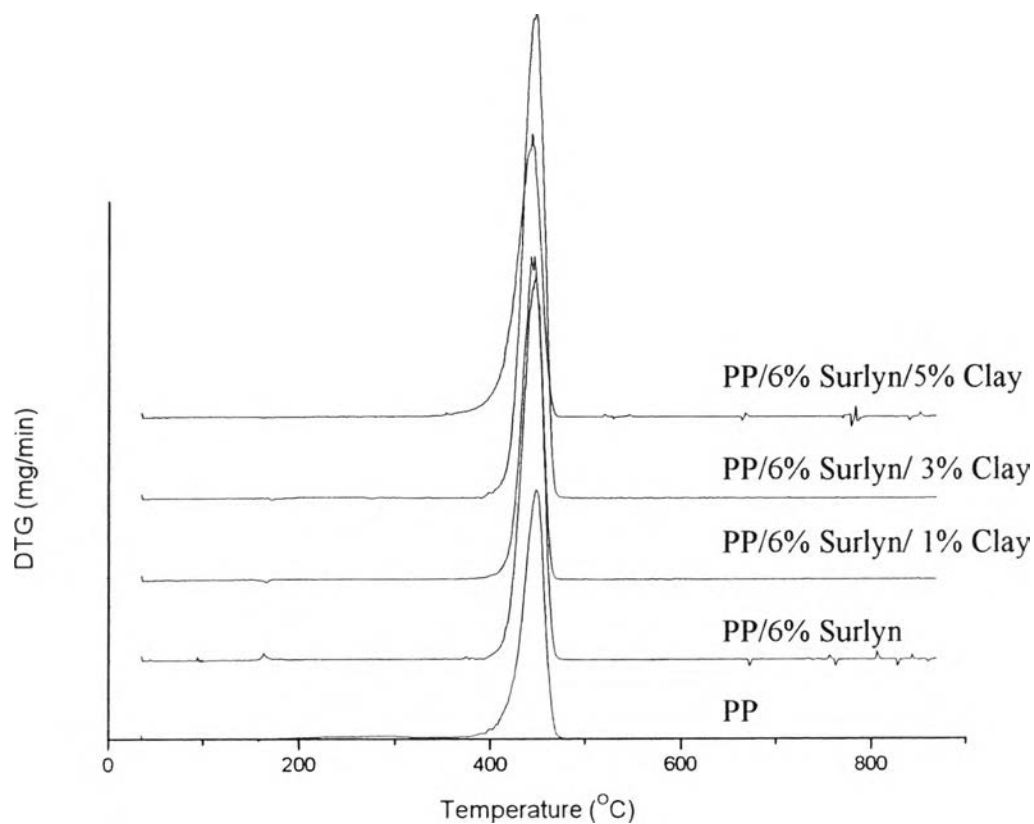
Figure 4.4 DTG curves of PP/organo-bentonite nanocomposite films
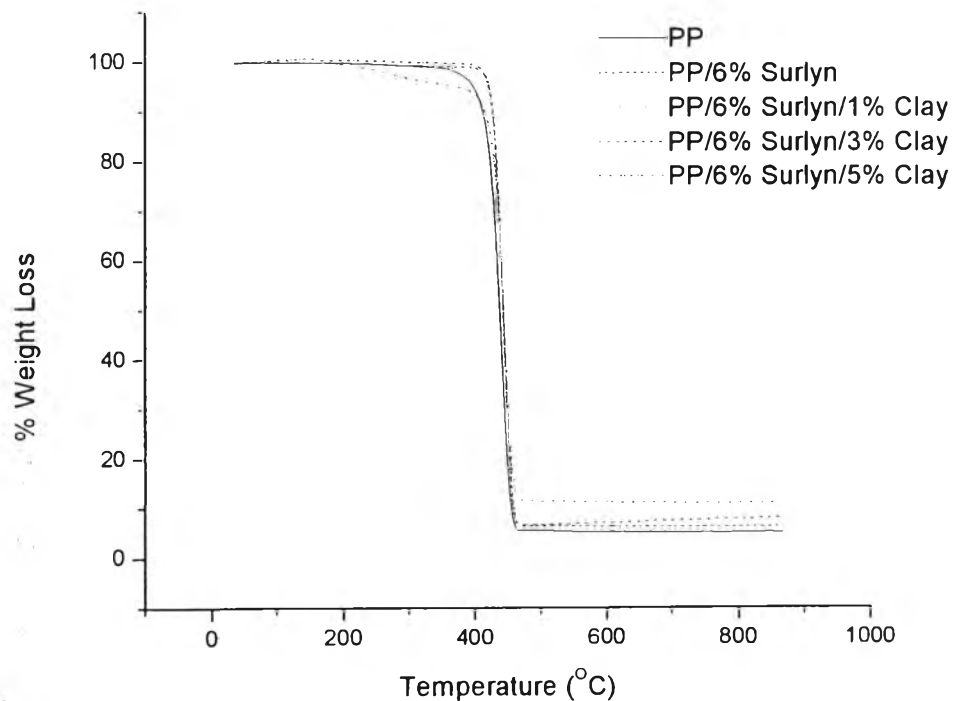
Figure 4.5 TGA curves of PP/organo-bentonite nanocomposite films

C. Crystallization behavior of PP/organo-modified bentonite nanocomposite films
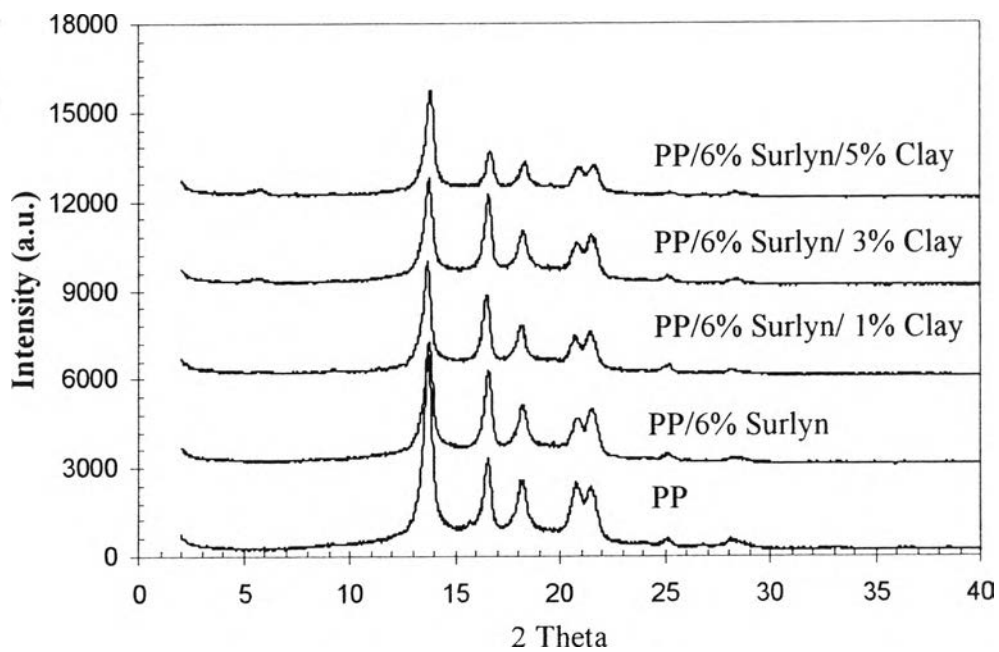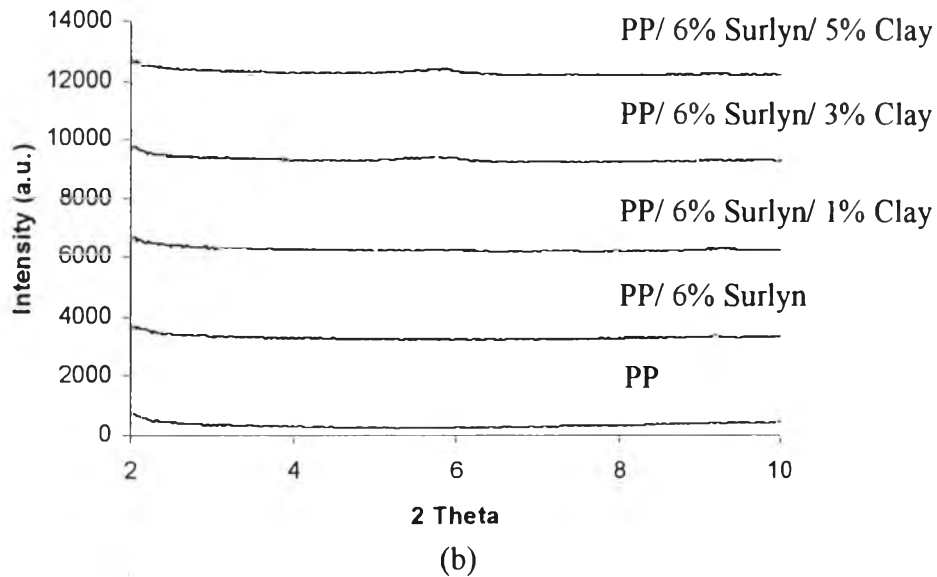

(a)

Figure 4.6 The XRD patterns of PP/organomodified bentonite nanocomposites films (a) 2θ = 2-40° and (b) 2θ = 2-10°.

The crystallization of nanocomposites films were determined by XRD within 2θ range between 2-40°, as shown in Fig. 4.6. The traditional PP shows five prominent which correspond to monoclinic α crystalline phase: α_1, α_2, α_3 and α_4 which is the (110), (040), (130) and (111, 041) reflection and corresponding to 2θ = 14.18, 16.98, 18.68, 21.24, and 21.94, respectively. The PP/organomodified-BTN nanocomposites films show the same corresponding peak with pristine PP, which mean the organomodified-BTN does not affect on the structure of PP crystal [7].

From Fig. 4.6 (b) the peaks correspond to the (001) reflections of the clay. It can not be observed in the XRD patterns of nanocomposite with 1% organo-modified bentonite suggesting that the silicate clay layers have a nearly exfoliated dispersion in the polymer matrix. When organo-modified bentonite contents in nanocomposite are increased the corresponding peak occurred at 2θ around 6° that means the intercalations of PP into the organo-modified bentonite layer are occurred [8].

D. Mechanical properties of PP/organo-modified bentonite nanocomposite films

The nanocomposite films were measured and concerned in Young's modulus, stress at break, and elongation at break. Figure 4.7 shows the Young's modulus of films, which was slightly increased to the hightest point at 1% organoclay. However, when clay content is 5% wt, Young's modulus is decreased due to the aggreagation of

the organomodified-BTN or remaining of some impurity in organoclay [9]. Moreover, the effect of organomodified-BTN on stress at break is shown in Figure 4.8. It is slightly reduced with increasing percent of organoclay content due to it lose the ability to transfer stress. According to Figure 4.9, the elongation at break is decreased, because the organobentonite obstructing the movement of PP along the applied force [10].
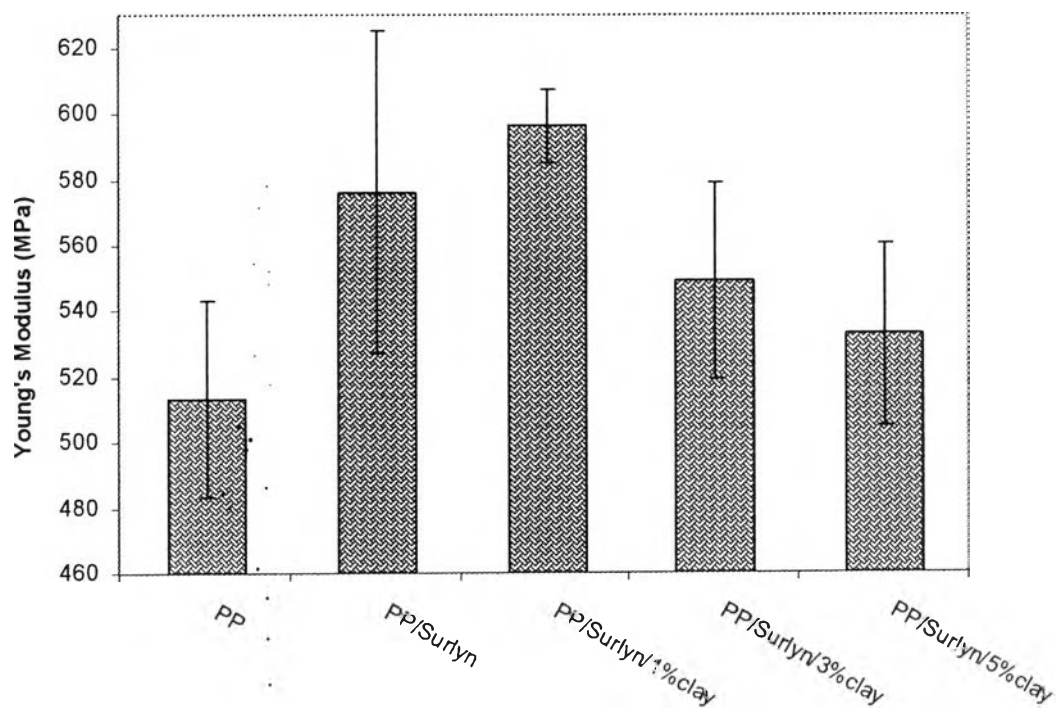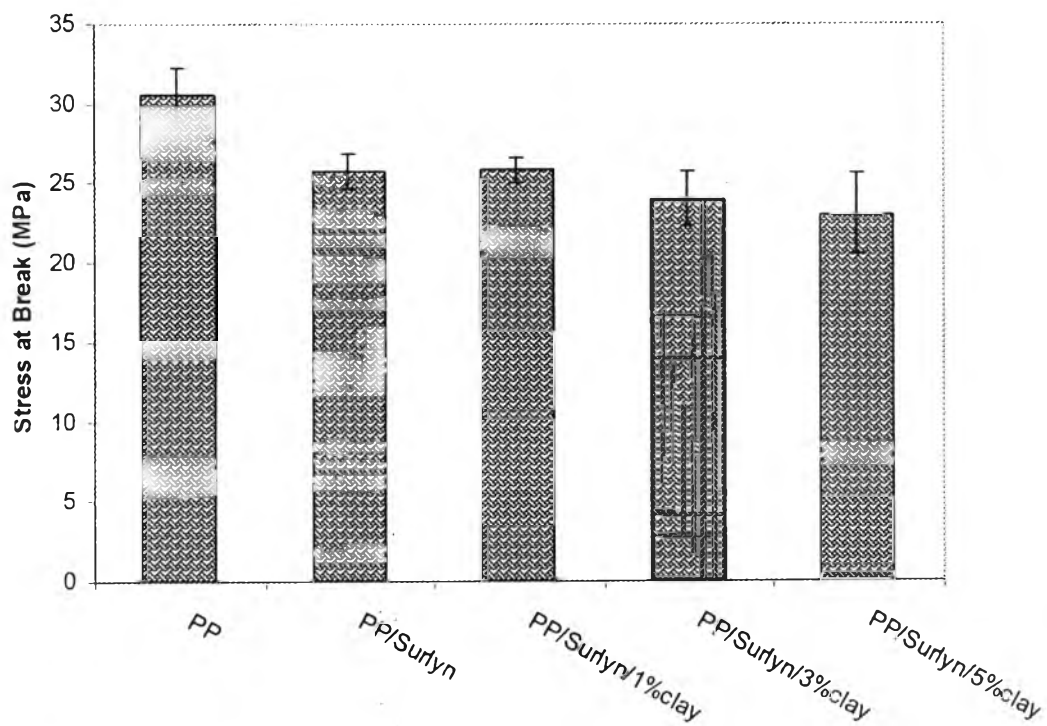

Figure 4.7 Young's modulus of PP/organomodified bentonite nanocomposite films

Figure 4.8 Stress at break of PP/organomodified bentonite nanocomposite films
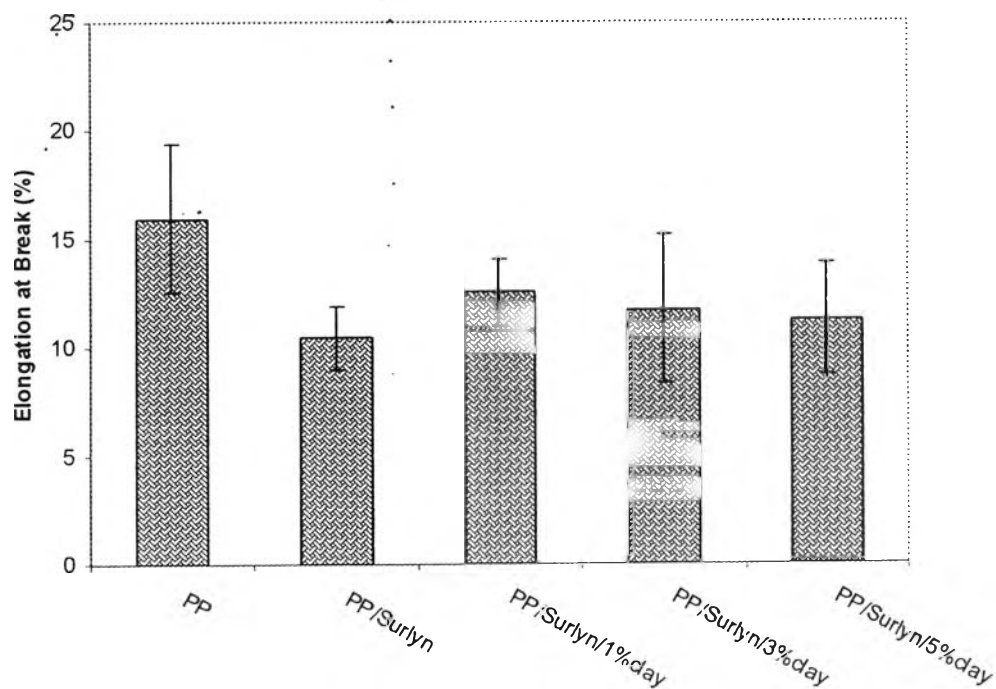

Figure 4.9 Elongation at break of PP/organo-bentonite nanocomposite films

F. Dispersion of organomodified-bentonite in nanocomposite films

Figure 4.10 shows the SEM images of organomodified-BTN in nanocomposites films. When percent of organoclay was increased, it reveals the accumulation of clay in the PP matrix as small nodules in the films. The incompatible between organoclay and PP matrix also affect the mechanical properties of films [11] mention before.
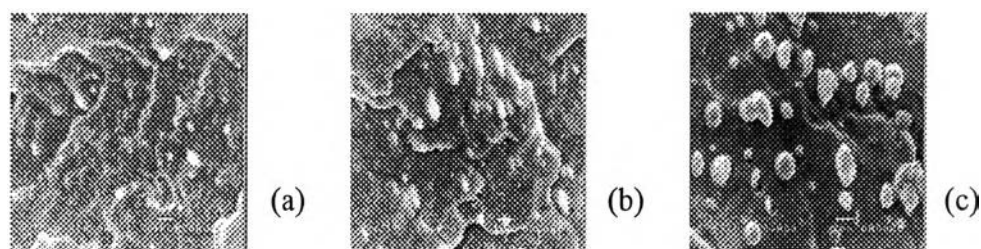

Figure 4.10 SEM images of nanocomposite pellets; (a) 1% Organoclay, (b) 3% Organoclay, (c) 5% Organoclay

G. Oxygen permeability of PP/organomodified bentonite nanocomposite films

Figure 4.11 is gas permeability which compared between traditional PP and nanocomposites films. The reduction of oxygen permeability due to clay is believed to increase the barrier properties by the combination of two phenomena: 1) creating a maze or tortuous path that retards the progress of the gas molecules through the matrix resin; 2) the decrease in area available for diffusion, a result of impermeable flakes replacing permeable polymer [12, 13]
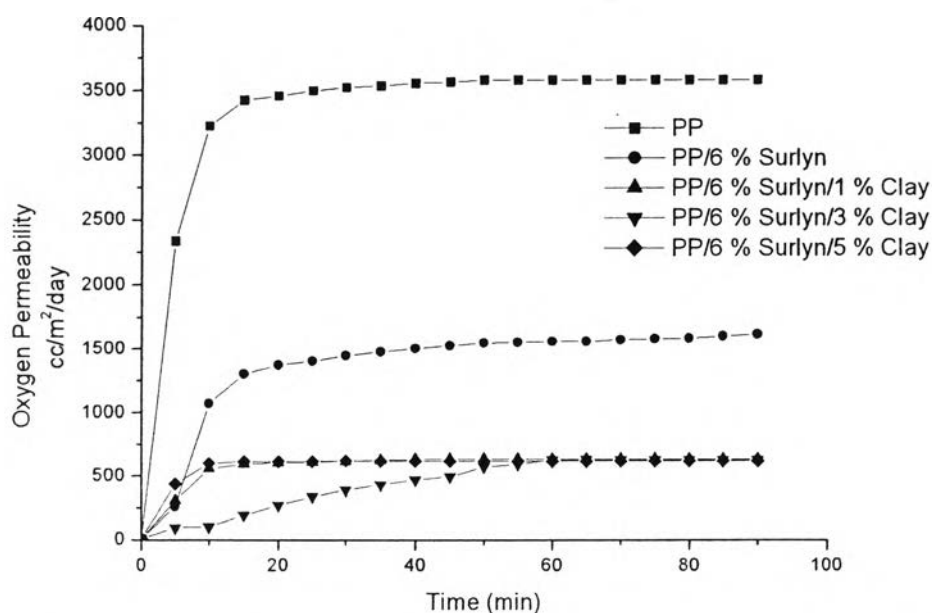

Figure 4.11 Oxygen permeability of PP and PP/organoclay nanocomposite films

4.5 Conclusions

The organomodified-BTN was obtained by treated clay, Na-BTN, with surfactant. When it mixed with PP and fabricate into active packaging films by vary the content of organomodified-BTN. The degradation temperature was increased by increasing the clay contents but melting temperature and crystallization temperature decreased due to the clay obstruct the packaging of PP chains. Moreover, the organo-modified-BTN can improve the Young's modulus of the films when increasing the organomodified-BTN content, however, tensile strength and elongation at break was slightly decreased because to it lose the ability to transfer stress. In addition, when the organo-BTN content in the packaging film increase, the agglomeration occurs as shown in the SEM images. These agglomerations drop the tensile properties of the films. Furthermore, the oxygen permeability reduces when increasing the organo-modified bentonite content due to the barrier properties of clay.

4.6 Acknowledgements

4.7 References

1   Varothai V., and Manuspiya H. (2006). Active packaging based on   ethylene scavenger PP / organomodified clay nanocomposites. *M.S. Thesis*, The Petroleum and Petrochemical College, Chulalongkorn University, Bangkok, Thailand.

2   J. Choy, S. Kwak, Y. Han and B. Kim. "New organo-montmorillonite complexes with hydrophobic and hydrophilic functions" *Materials Letters*, **33**(1997), 143-147.

3   Y. Xi, Z. Ding and R.L. Frost. "Structure of organo-clays-an X-ray diffraction and thermogravimetric analysis study" *Colloid and Interface Science*, **227**(2004), 116-120.

4   K. Kosuge. "Layered polysilicate gas adsorption properties and dispersion of the particles" *Clay Science Society of Japan*, **33**(1994), 215-222.

5   F. Wypych. K.G. Satyanarayana. "Clay Surfaces: Fundamentals and Applications" *Interface Science and Technology*, **1**(2004), 290-345.

6   S. Parija, S.K. Nayak, S.K. Verma, and S.S. Tripathy. "Studies on physico-mechanical Properties and thermal characteristics of polypropylene/layer silicate nanocomposites" *Polymer Composites*, **25**(2004), 646-652.

7   H. Qin, S. Zhang, C. Zhao, G. Hu, and M. Yang. "Flam retardant mechanism of polymer/clay nanocomposites based on polypropylene " *Polymer*, **46**(2005), 8386-8395.

8   F. Chiu, S.Lai, J. Chen, and P. Chu. "Combined effect of clay modification and compatibilizers on the formation and physical properties of melt-mixed polypropylene/clay nanocomposites " *Polymer Science*, **42**(2004), 4139-4150.

9   F.G. Ramos, T.A. Melo, M.S. Rabello, and S.M. Silva. "Thermal stability of nanocomposites based on polypropylene and bentonite" *Polymer Degradation and Stability*, **89**(2005), 383-392.

10 N. Othman, H. Ismail and M. Mariatti "Effect of compatibilizers on mechanical and thermal properties of bentonite filled polypropylene composites" *Polymer Degradation and Stability*, **91**(2006), 1761-1774.

11 L. Szazdi, B. Pkanszky Jr, G.J. Vancso, and B. Pukanszky. "Quantitative estimation of the reinforcing effect of layered silicates in PP nanocomposites" *Polymer*, **47**(2006), 4638-4648.

12 F. Masoud, D. Susan, S. Zahra, M. Mohsen. "Gas barrier properties of PP/EPDM blend nanocomposites" *Journal of Membrane Science*, **282**(2006), 142-148.

13 R. Suprakas, O. Masami. "Polymer/layered silicate nanocomposites: a review from preparation to processing" *Progress in Polymer Science*, **28**(2003), 1539-1641